

Comparative study on the cellular activities of osteoblast-like cells and new bone formation of anorganic bone mineral coated with tetra-cell adhesion molecules and synthetic cell binding peptide

Hyeon-Seok Yu¹, Woo-Chang Noh^{1,2}, Jin-Woo Park¹, Jae-Mok Lee¹, Dong-Jun Yang³, Kwang-Bum Park³, Jo-Young Suh^{1,2,*}

¹Department of Periodontology, ²Institute for Hard Tissue and Bio-Tooth Regeneration, Kyungpook National University School of Dentistry, Daegu, Korea

³Megagen Implant, Gyeongsan, Korea

Purpose: We have previously reported that tetra-cell adhesion molecule (T-CAM) markedly enhanced the differentiation of osteoblast-like cells grown on anorganic bone mineral (ABM). T-CAM comprises recombinant peptides containing the Arg-Gly-Asp (RGD) sequence in the tenth type III domain, Pro-His-Ser-Arg-Asn (PHSRN) sequence in the ninth type III domain of fibronectin (FN), and the Glu-Pro-Asp-Ilu-Met (EPDIM) and Tyr-His (YH) sequence in the fourth fas-1 domain of β ig-h3. Therefore, the purpose of this study was to evaluate the cellular activity of osteoblast-like cells and the new bone formation on ABM coated with T-CAM, while comparing the results with those of synthetic cell binding peptide (PepGen P-15).

Methods: To analyze the cell viability, 3-(4,5-dimethylthiazol-2-yl)-2,5-diphenyltetrazolium bromide assay was performed, and to analyze gene expression, northern blot was performed. Mineral nodule formations were evaluated using alizarin red stain. The new bone formations of each group were evaluated using histologic observation and histomorphometric analysis.

Results: Expression of alkaline phosphatase mRNA was similar in all groups on days 10 and 20. The highest expression of osteopontin mRNA was observed in the group cultured with ABM/P-15, followed by those with ABM/T-CAM and ABM on days 20 and 30. Little difference was seen in the level of expression of collagen type I mRNA on the ABM, ABM/T-CAM, and ABM/P-15 cultured on day 20. There were similar growth and proliferation patterns for the ABM/T-CAM and ABM/P-15. The halo of red stain consistent with Ca^{2+} deposition was wider and denser around ABM/T-CAM and ABM/P-15 particles than around the ABM particles. The ABM/T-CAM group seemed to have bone forming bioactivity similar to that of ABM/P-15. A complete bony bridge was seen in two thirds of the defects in the ABM/T-CAM and ABM/P-15 groups.

Conclusions: ABM/T-CAM, which seemed to have bone forming bioactivity similar to ABM/P-15, was considered to serve as effective tissue-engineered bone graft material.

Keywords: Bone substitutes, Cell adhesion molecules, Cell survival.

INTRODUCTION

Implantation of bone graft materials to stimulate bone deposition has been used in periodontal therapy since the 1970s.

Recently different graft materials, including demineralized and non-mineralized freeze-dried bone allografts, various types of natural and synthetic hydroxyapatite, ceramics, calcium carbonate, and synthetic polymers have been utilized

Received: Sep. 9, 2011; **Accepted:** Oct. 22, 2011

***Correspondence:** Jo-Young Suh

Department of Periodontology, Kyungpook National University School of Dentistry, 2177 Dalgubeol-daero, Jung-gu, Daegu 700-421, Korea

E-mail: jysuh@knu.ac.kr, Tel: +82-53-600-7521, Fax: +82-53-427-3263

as bone graft materials. Bone grafts have long been used in reconstructive surgery with the aim of increasing the bone volume in the previous defect area. An ideal bone graft or bone substitute material should presumably have the following characteristics: sterility, not eliciting any immunological reaction, osteoconductivity or osteoinductivity, favorable clinical handling, ability to be resorbed and replaced by bone, availability in sufficient quantities, and low cost [1].

The autogenous bone graft is the material most likely to possess both osteoconductive and osteoinductive properties [2,3]. However, in an attempt to avoid separate surgical procedures involving a remote donor site and reduce postsurgical pain, patient inconvenience, operating time and cost, clinicians have increased their use of alternative grafting materials.

The recent development of tissue engineering makes it possible to envision the association of autologous cell and/or proteins that promote cell adhesion with osteoconductive material to create osteoinductive materials. Based on this concept, commercially available synthetic cell binding peptide (PepGen P-15, Dentsply Friadent CeraMed, Lakewood, CO, USA) developed. PepGen P-15 is biomimetic biomaterial composed of anorganic bone mineral (OsteoGraf/N-300, Dentsply Friadent CeraMed) and a synthetic peptide (P-15) that mimics the cell-binding domain of type I collagen responsible for cell migration, proliferation, and differentiation [4]. A synthetic 15-residue peptide, which is analogous to the sequence $^{766}\text{GTPGPQGIAGQRGVV}^{780}$ in the $\alpha 1$ (I) chain, is related to a biologically active portion of type I collagen [5].

Theoretical studies have shown that the central GIAG sequence of this P-15 sequence has a high potential for a stable β -bend [6]. It has been demonstrated *in vitro* that the anorganic bone mineral/P-15 (ABM/P-15) enhances the attachment of cells and provides an environment that is permissive for cell migration, cell differentiation, and morphogenesis [4,7,8]. In addition, experimental studies have reported that the use of the materials in small and large bony defects enhances new bone formation [9-11].

Recently, we reported [12] that the cell adhesion molecule tetra-cell adhesion molecule (T-CAM) markedly enhanced the differentiation of osteoblast-like cells grown on ABM. T-CAM is composed of recombinant peptides containing the Arg-Gly-Asp (RGD) sequence in the tenth type III domain, the Pro-His-Ser-Arg-Asn (PHSRN) sequence in the ninth type III domain of fibronectin (FN), and the Glu-Pro-Asp-Ilu-Met (EPDIM) and Tyr-His (YH) sequence in the fourth fas-1 domain of β ig-h3. The RGD peptide signaling domain derived from fibronectin interacts with several cell surface integrins, the major one being $\alpha 5\beta 1$ [13,14], and promotes osteoblast adhesion [15]. The PHSRN sequence within the ninth type III

domain serves as a synergistic site that enhances the binding affinity of the RGD sequence [16]. β ig-h3 induced by TGF- β is an ECM protein that has four internal repeat domains named fas-1 [17,18] and has been considered to promote cell adhesion and spreading through the $\alpha 3\beta 1$ and $\alpha v\beta 5$ integrin mediating EPDIM and YH sequences within the fourth fas-1 domain [19,20]. Therefore, both sequences of RGD and PHSRN in T-CAM are recognized by integrin $\alpha 5\beta 1$ in osteoblast-like cells [21]. EPDIM and YH in T-CAM may be recognized by integrin $\alpha 3\beta 1$ and $\alpha v\beta 5$ in osteoblast-like cells [19,20].

Therefore, the purpose of this study was to evaluate the cellular activity of osteoblast-like cells and new bone formation on ABM coated with T-CAM, while comparing the results with those of ABM coated with a synthetic peptide which mimics the cell-binding domain of type I collagen, PepGen P-15.

MATERIALS AND METHODS

Experimental materials

PepGen P-15, anorganic bone mineral (OsteoGraf/N-300) coated with synthetic P-15, which is analogous to the sequence $^{766}\text{GTPGPQGIAGQRGVV}^{780}$ in the $\alpha 1$ (I) chain of type I collagen and ABM in a particulate form (OsteoGraf/N-300) and OsteoGraf/N-300 for the carrier of T-CAM were obtained from Dentsply Friadent CeraMed.

Peptide synthesis

T-CAM is a fusion protein consisting of the 9th and 10th type III domains of fibronectin and the 4th fas-1 domain of β ig-h3. A fragment of fibronectin cDNA, encoding amino acids 1,330 to 1,513 was generated by polymerase chain reaction and restricted to the Nde I and Nsi I sites. The Nde I/Nsi I fragment of fibronectin cDNA was inserted into the EcoRV sites of the 4th fas-1 domain of β ig-h3 [19]. Plasmid constructs encoding T-CAM were transformed into BL21 (DE3) for expression. Overnight bacterial culture was induced by 1 mM IPTG for 3 hours and T-CAM protein was purified using Ni-NTA resin (Qiagen, Hilden, Germany) according to the manufacturer's recommendations [19].

Preparation of ABM/T-CAM

For study of the effect of T-CAM on cellular activity of osteoblast-like cells and new bone formation in rabbit calvarial defects, the peptide was absorbed into ABM by incubating 0.5 g ABM for 24 hours in a concentration of 100 $\mu\text{g/mL}$ T-CAM. The incubation was carried out at room temperature with gentle shaking to ensure equilibration of the peptide with all the exposed surfaces of the microporous ABM. Following incubation, the ABM was washed three times by shaking with a

5× volume of phosphate buffered saline (PBS) over a 24 hours period to remove unabsorbed peptide. The ABM powder was collected and dried in a dry oven. ABM with T-CAM absorbed peptide was generated using sterilized preparations.

Osteoblast culture on ABM, ABM/T-CAM, and ABM/P-15

We used the mouse calvaria-derived MC3T3-E1 osteoblast-like cell line for this study. MC3T3-E1 cells were cultured in alpha-modified Eagle's medium (Gibco, Grand Island, NY, USA) supplemented with 10% fetal bovine serum (FBS, Gibco) and 500 unit/mL penicillin (Kunwha Pharmaceutical Co., Seoul, Korea), 500 µg/mL streptomycin (Dong-A Pharmaceutical Co., Seoul, Korea) and cultured in an atmosphere of 100% humidity, 5% CO₂, and 37°C. Cells were grown in 10% FBS containing 10 mM β-glycero-phosphate (Sigma-Aldrich Co., St. Louis, MO, USA), 50 µg/mL of ascorbic acid and 100 nM dexamethasone in 100 mm dishes or 24 well plates (Corning Inc., Corning, NY, USA) for the experiments. The medium was changed every 3 days.

The experimental groups were classified as follows:

ABM: OsteoGraf/N-300 particles in polystyrene petri dishes

ABM/T-CAM: OsteoGraf/N-300 particles absorbed in T-CAM in polystyrene petri dishes

ABM/P-15: OsteoGraf/N-300 particles absorbed in P-15 (PepGen P-15) in polystyrene petri dishes

MTT assay for viable cell numbers

MTT (3-[4,5-dimethylthiazol-2yl]-2, 5 diphenyltetrazolium bromide; thiazolyl blue) assay is transformed by mitochondrial dehydrogenases into formazan, enabling mitochondrial activity and cell viability to be assessed. The cultured cells were seeded at an initial density of 2×10^4 cells/well on each well containing each particle of the 24 well plate. Three kinds of particles (30 mg/well)–ABM, ABM/T-CAM and ABM/P-15–were used in each group. The cells were cultured in an atmosphere of 100% humidity, 5% CO₂, and 37°C for 1, 4, and 7 days. They were then removed from the medium and washed with PBS two times. Then, 250 µL of MTT solution prewarmed to 37°C was added to each well and incubated for 3 hours in the same condition and 750 µL of dimethyl sulfoxide (DMSO) and 250 µL of glycine buffer were added. The solution was transferred to 96-well plates that did not contain the particles. The optical density was measured at a wavelength of 570 nm by an enzyme-linked immunosorbent assay (ELISA) reader (Precision Microplate Reader, Molecular Devices Co., Sunnyvale, CA, USA).

Gene expression for bone matrix protein

The cultured cells were seeded at an initial density of 8×10^4

cells/well. The wells contained 150 mg/well of particles from the 100 mm petri dishes. The cells were cultured in an atmosphere of 100% humidity, 5% CO₂, and 37°C for 10 and 20 days for alkaline phosphatase (ALP) and during 10, 20, and 30 days for osteopontin (OPN) and collagen type I (Col I).

Total RNA was extracted from the cultured cells by using a modified acid phenol method. Ten µg of total RNA was heated to 65°C for 15 minutes in 50% formamide, 0.02% formaldehyde, 40 nM MOPS (3-[N-morpholino]propanesulfonic acid), 10 mM sodium acetate, 1 mM ethylenediaminetetraacetic acid (EDTA), and 0.1 mg/mL ethidium bromide prior to gel electrophoresis on 1% agarose, 55% formaldehyde, 40 mM MOPS, 10 mM sodium acetate, and 1 mM EDTA. The RNA was blotted onto Hybond-N+Membranes (Amersham Biosciences, Uppsala, Sweden) in 20X SSC. The RNA was air-dried and then cross-linked by exposure to ultraviolet light. The probes were labelled with [α-³²P]-dCTP by a Megaprime DNA labeling system kit (Amersham Biosciences). Prehybridization and hybridization were performed by using the Express Hyb solution (Clontech, Mountain View, CA, USA). After hybridization, the membrane was washed in 2X SSC - 0.1% sodium dodecyl sulfate (SDS) at room temperature and then in 0.1X SSC/0.1% SDS at 55°C, and exposed to Agfa X-ray film at -70°C with intensifying screens.

Staining with alizarin red for mineralization

Red staining with alizarin red is an indicator of mineralization [22]. MC3T3-E1 cell cultures on ABM, ABM/T-CAM, and ABM/P-15 were prepared for staining by removing the medium, washing the cells with PBS, and fixing them in 2% paraformaldehyde for 30 minutes at 4°C following which the cells were gently washed with H₂O. The cells were stained in a solution of 1% alizarin red S, pH 4.2 for 10 minutes at room temperature, and then, the cells were washed with H₂O two times. The samples were air dried, and were then examined and photographed in a light microscope.

Animal study for evaluation of new bone formation

Eight adult male New Zealand White rabbits weighing 3.0 to 3.5 kg were used in this study. This experiment was approved by the Institutional Animal Care and Use Committee of Kyungpook National University Hospital, Daegu, Korea. The animals were anesthetized preoperatively with an intramuscular injection of ketamine hydrochloride of 44 mg/kg of body weight (Ketalar, Yuhan, Seoul, Korea) and xylazine of 7 mg/kg of body weight (Rompun, Bayer Korea Ltd, Seoul, Korea). Two full thick skull defects were made in the parietal bones with a trephine bur (3i Implant Innovations Inc., Palm Beach Gardens, FL, USA). The defects were rinsed with sterile saline and then filled with the ABM/T-CAM and ABM/P-15

graft materials.

The defects were evaluated at 4 weeks after implantation. The specimens were fixed with the mixture of 4% paraformaldehyde in 0.1 M PBS. After fixation, the specimens were sectioned at 5 μ m with a microtome and stained with Masson's trichrome.

Statistical analysis

The data analysis of this study was analyzed using the statistical software package (SAS, SAS Institute Inc., Cornelius, NC, USA). In the cellular activity of osteoblast-like cells, the Student-Newman-Keuls test was used to determine the statistical significance of the three groups. All values are expressed as means \pm standard deviations. Statistical significance was established at $P < 0.01$.

RESULTS

MTT assay for cellular viability

Cell proliferation and viability in the ABM, ABM/T-CAM, and ABM/P-15 groups were measured by MTT assay at 1, 4, and 7 days and the results are presented in Fig. 1. The MTT assay indicated the increases in viable cell numbers of the ABM, ABM/T-CAM, and ABM/P-15 groups according to the time. The cell numbers were significantly higher in ABM/T-CAM and ABM/P-15 groups at 4 and 7 days ($P < 0.01$), compared to the ABM group. We also observed these results on hematoxylin and eosin stains at 4 day culture (Fig. 2).

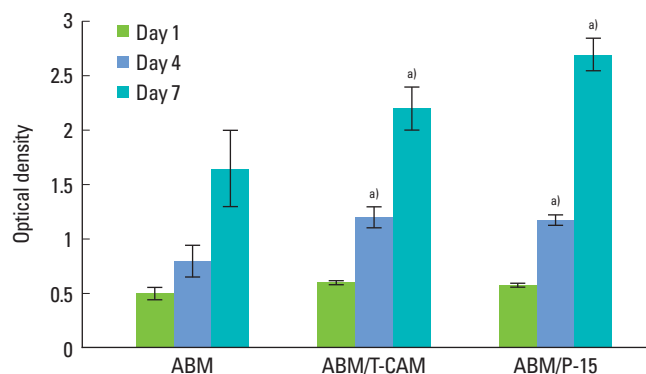


Figure 1. Optical density measured after culture for 1, 4, and 7 days at a wavelength of 579 nm by an enzyme-linked immunosorbent assay reader ($n=3$ in each group). The optical density of anorganic bone mineral/tetra-cell adhesion molecule (ABM/T-CAM) and ABM/P-15 was significantly higher than ABM alone on days 4 and 7. ^{a)}A statistically significant difference as compared with ABM ($P < 0.01$). ABM: OsteoGraf/N-300 particles in polystyrene petri dishes, ABM/T-CAM: OsteoGraf/N-300 particles absorbed T-CAM in polystyrene petri dishes, ABM/P-15: OsteoGraf/N-300 particles absorbed P-15 (PepGen P-15) in polystyrene petri dishes.

The expression of ALP mRNA, OPN mRNA, and Col I mRNA

Fig. 3 shows the expression of alkaline phosphatase mRNA of the cells cultured with the ABM, ABM/T-CAM, and ABM/P-15 on days 10 and 20. Expression of alkaline phosphatase mRNA was also similar in all groups on days 10 and 20. The groups cultured on day 10 showed higher expression of alkaline phosphatase mRNA than the groups cultured on day 20.

Fig. 4 shows the expression of osteopontin mRNA and collagen type I mRNA of the cells cultured with the ABM, ABM/T-CAM, and ABM/P-15 on days 10, 20, and 30. Among the experimental groups, the highest expression of osteopontin mRNA was observed in the group cultured with ABM/P-15, followed by those with ABM/T-CAM and ABM on day 20. Furthermore, the expression of osteopontin mRNA was higher in all groups cultured on day 10 and 20 than in all groups cultured on day 30. The expression of OPN mRNA on ABM/T-CAM and ABM/P-15 was similar to that on ABM at 10 days culture. Although little difference was seen in the level of expression of collagen type I mRNA on the ABM, ABM/T-CAM, and ABM/P-15 cultured on day 20, greater expression was observed in the 30 day culture on ABM/T-CAM and ABM/P-15 than on ABM.

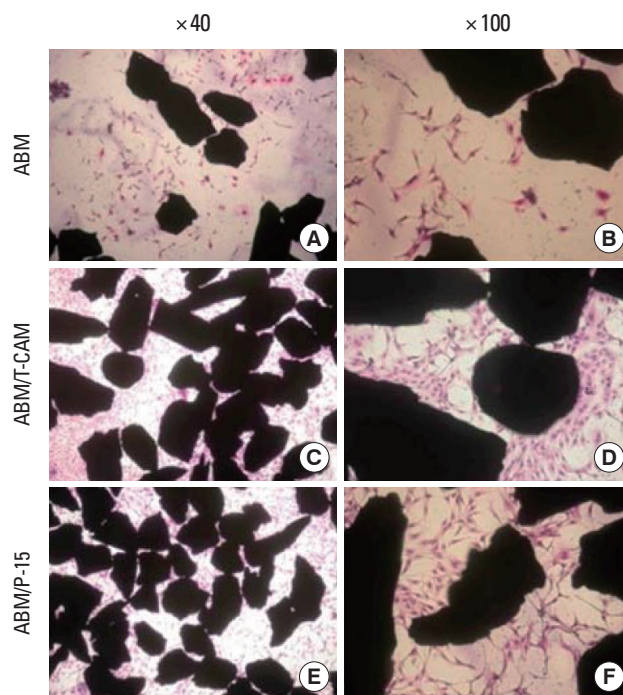


Figure 2. Cellular viability of anorganic bone mineral (ABM), ABM/tetra-cell adhesion molecule (ABM/T-CAM), and ABM/P-15 at 4 day culture stained by H&E. (A) ABM ($\times 40$), (B) ABM ($\times 100$), (C) ABM/T-CAM ($\times 40$), (D) ABM/T-CAM ($\times 100$), (E) ABM/P-15 ($\times 40$), (F) ABM/P-15 ($\times 100$). MC3T3-E1 cells were attached in remarkably great numbers on ABM/T-CAM and ABM/P-15 than on ABM.

Staining with alizarin red

The growth and mineralization pattern of osteoblast-like cells cultured with ABM, ABM/T-CAM and ABM/P-15 was examined using a phase-contrast microscope after staining with alizarin red S at 30 day culture (Fig. 5). There were similar growth and proliferation patterns for the ABM/T-CAM and ABM/P-15. In these groups, the cells formed multicellular layers around the graft material and interparticular bridges between them. Multicellular layers and interparticular bridges were also observed in cultures with ABM, but only in a few cases.

Very strong staining with the dye was seen in osteoblast-like cell cultures on ABM, ABM/T-CAM, and ABM/P-15. Fig. 5A, 5C, and 5E show staining around isolated ABM, ABM/T-CAM, and ABM/P-15 particles. The halo of red stain consistent with Ca²⁺ deposition was wider and denser around the ABM/T-CAM and ABM/P-15 particles than around the ABM particles.

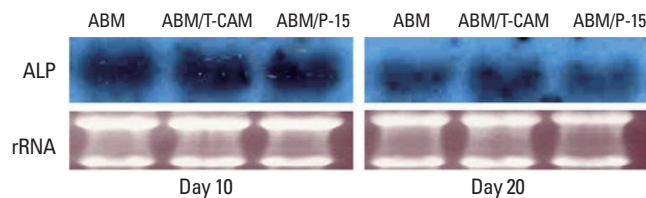


Figure 3. Gene expression of alkaline phosphatase (ALP) of MC₃T₃-E1 cells cultured on anorganic bone mineral (ABM), ABM/tetra-cell adhesion molecule (ABM/T-CAM), and ABM/P-15 for 10 and 20 days. The ALP activity of MC₃T₃-E1 cells on ABM/T-CAM and ABM/P-15 was similar to that of ABM. ABM: OsteoGraf/N-300 particles in polystyrene petri dishes, ABM/T-CAM: OsteoGraf/N-300 particles absorbed on T-CAM in polystyrene petri dishes, ABM/P-15: OsteoGraf/N-300 particles absorbed on P-15 (PepGen P-15) in polystyrene petri dishes.

New bone formation in rabbit calvarial defects

The histologic findings at 4 weeks of healing are shown in Fig. 6. The ABM/T-CAM group seemed to have similar bone

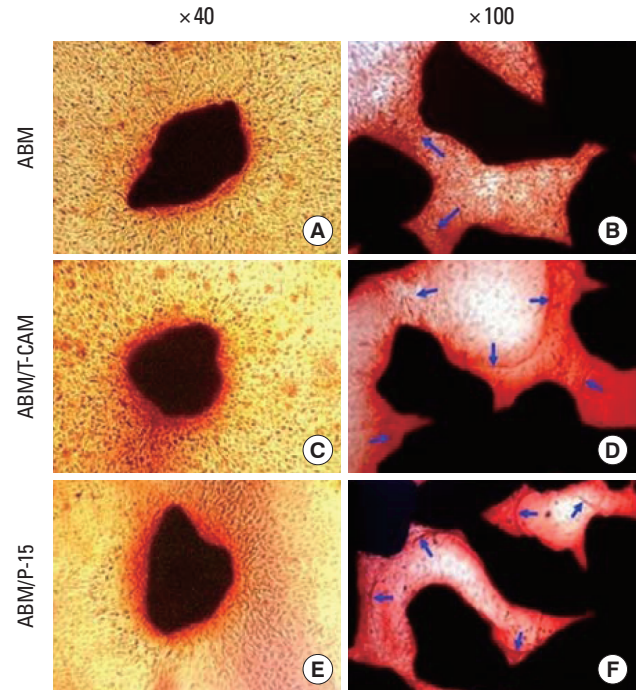


Figure 5. Staining with alizarin red S on anorganic bone mineral (ABM), ABM/tetra-cell adhesion molecule (ABM/T-CAM), and ABM/P-15 at 30 day culture. (A) ABM (×40), (B) ABM (×100), (C) ABM/T-CAM (one particle ×100), (D) ABM/T-CAM (particles ×100), (E) ABM/P-15 (one particle ×100), (F) ABM/P-15 (particles ×100). There were similar growth and proliferation patterns for ABM/T-CAM and ABM/P-15. In these groups, the cells formed multicellular layers around the graft material and interparticular bridges between them. Multicellular layers were also observed in the cultures with ABM, but fewer. The halo of red stain consistent with Ca²⁺ deposition is wider and denser around the ABM/T-CAM and ABM/P-15 particles than around the ABM particles.

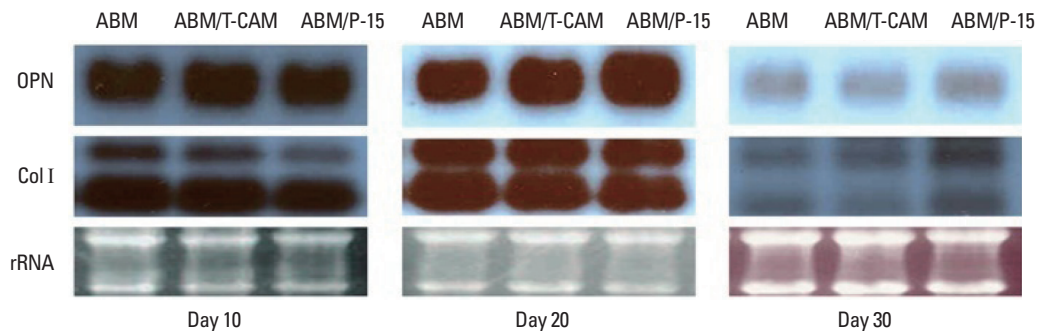


Figure 4. Gene expression of osteopontin (OPN) and α₁ (I) collagen (Col I) of MC₃T₃-E1 cells cultured on anorganic bone mineral (ABM), ABM/tetra-cell adhesion molecule (ABM/T-CAM), ABM/P-15 for 10, 20, and 30 days. The expression of OPN mRNA on ABM/T-CAM and ABM/P-15 was similar to that of ABM at 10 days culture, but was remarkably higher on ABM/T-CAM and ABM/P-15 than ABM at 20 days culture. The expression of Col 1 mRNA on ABM/T-CAM and ABM/P-15 was similar to that of ABM at 20 days culture. ABM: OsteoGraf/N-300 particles in polystyrene petri dishes, ABM/T-CAM: OsteoGraf/N-300 particles absorbed T-CAM in polystyrene petri dishes, ABM/P-15: OsteoGraf/N-300 particles absorbed P-15 (PepGen P-15) in polystyrene petri dishes.

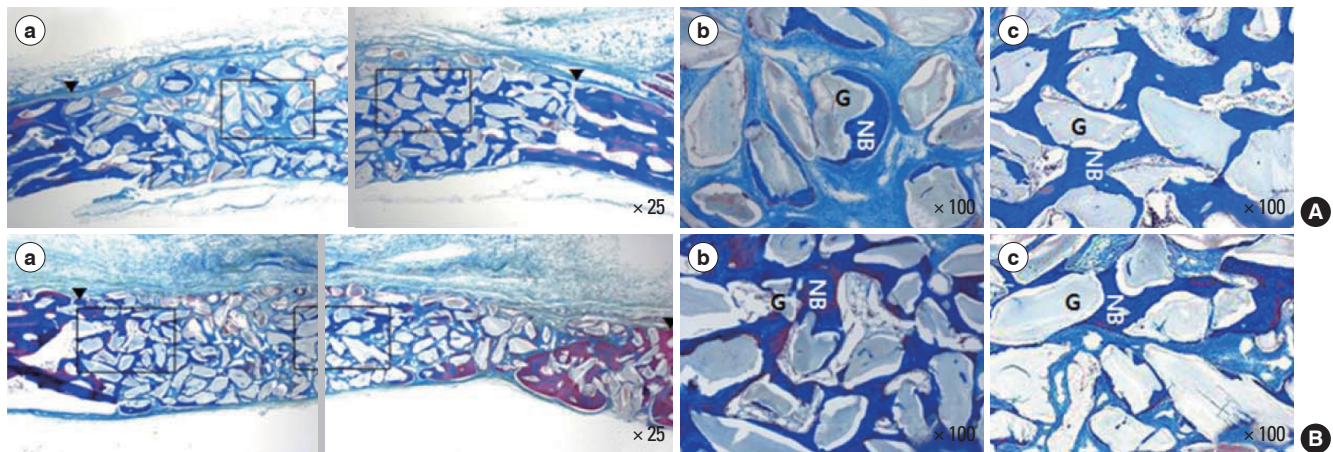


Figure 6. Histologic findings of defects filled with anorganic bone mineral/tetra-cell adhesion molecule (ABM/T-CAM) (A) and ABM/P-15 (B) at 4 weeks (Masson's Trichrome stain). (a) Whole findings ($\times 25$), (b) High magnification ($\times 100$), (c) High magnification ($\times 100$). (\blacktriangledown : margin defect, G: graft material, NB: new bone). A complete bony bridge was seen in two thirds of the defects in the ABM/T-CAM and ABM/P-15 groups (A-a and b). Newly formed bone was seen in direct apposition to the graft material (A-b). The new mineralized tissue consisted of woven bone characterized by a high number of randomly distributed large osteocytes and by irregularly arranged fiber bundles within the new bone matrix (A-c). At the margin of the defect, the new bone that had emerged from the old bone was mature (B-b). Among the graft materials, the direct union of new bone was favorably observed (A and B-c).

forming bioactivity to the ABM/P-15 group. A complete bony bridge was seen in two thirds of the defects in the ABM/T-CAM and ABM/P-15 groups (Fig. 6A-a and B-a). Newly formed bone was seen in direct apposition to the bone particles (Fig. 6A-b). The new mineralized tissue consisted of woven bone characterized by a high number of randomly distributed large osteocytes and by irregularly arranged fiber bundles within the new bone matrix (Fig. 6A-c and B-c). Among the particles, the direct union of new bone was favorably observed (Fig. 6A-c and B-c). At the defect margin, the new bone that had emerged from the old bone was mature (Fig. 6B-b).

DISCUSSION

Bone formation is related to the adherence of osteoblasts to graft material. The adherence can be enhanced by coating graft materials with certain cell binding peptides of the extracellular matrix. The interaction of osteoblasts with the extracellular matrix proteins represents essential environmental signals necessary for regulating proliferation and differentiation of osteoblasts [23]. This interaction is mediated primarily through the integrin family [24]. Osteoblasts express a wide array of integrin heterodimers, both *in vivo* and *in vitro*, particularly those interacting with the extracellular matrix proteins of bone [25-27]. A number of investigators report the expression of a broad range of integrin subunits in bone cells, including $\alpha 1\beta 1$, $\alpha 2\beta 1$, $\alpha 3\beta 1$, $\alpha 5\beta 1$, $\alpha v\beta 3$, and $\alpha v\beta 5$ [25,26,28]. Both sequences of RGD and PHSRN in fibronectin are recognized by integrin $\alpha 5\beta 1$ in osteoblast-like cells [21]. EPDIM and YH in 4th fas-1 domain of β ig-h3 may be recognized by

integrin $\alpha 3\beta 1$ and $\alpha v\beta 5$ in osteoblast-like cells [19,20].

Collagen also modulates cell differentiation mechanically and chemically [7,29]. The involvement of a specific chain of 15 peptides in the processes of cell differentiation was demonstrated for the first time by Qian and Bhatnagar [4] in 1996. This amino acid sequence (766-780 of the $\alpha 1$ chain of the type 1 collagen) is responsible for cell bonding and the initiation of a cascade of events that lead to the formation of new bone, and is also referred to as P-15. The ABM/P-15 bone graft material has been shown *in vitro* to enhance the attachment of cells [4,7,29], and to enhance bone formation within a shorter time interval compared with the composite graft material of HA and autogenous bone in the human maxillary sinus evaluation procedure [30].

We synthesized T-CAM, which is the recombinant protein containing an RGD sequence in the tenth type III domain and a PHSRN sequence in the ninth type III domain of fibronectin, and a YH sequence and EPDIM sequence in the fourth fas-1 domain of β ig-h3, and we evaluated the cellular activity of osteoblast-like cells and new bone formation to ABM coated with T-CAM, while comparing the results with those of ABM coated with a synthetic peptide (P-15) that mimics the cell-binding domain of type I collagen, PepGen P-15.

Using the MTT assay for the cellular viability of osteoblast-like cells, a statistical difference in cell viability was observed when osteoblast-like cells were cultured for 4 and 7 days on ABM/T-CAM and ABM/P-15 compared to ABM. It was concluded that the increase in cellular viability of ABM/T-CAM was due to four cellular adhesion molecules absorbed to hy-

droxyapatite, which was similar to another study [31]. They reported that the proliferation of periodontal ligament cells in FN fragments containing FN type III ninth-tenth domain fragments did not differ statistically from those in FN. The results on ABM/P-15 might be explained by the mechanism of enhanced cell proliferation resulting from the type I collagen binding of the P-15 peptide [4,7,29].

In order to study the osteoblastic characteristics of cultured cells, we examined the expression of several genes implicated in osteoblastic differentiation. The expression of ALP mRNA was also similar in all groups on days 10 and 20. The groups cultured on day 10 showed a higher expression of ALP mRNA than the groups cultured on day 20. It was demonstrated that osteoblast-like cells reached the highest ALP activity level after 7 to 10 days [32]. Also, the ALP decrease could represent a maturation of osteoblasts [33]. Col I is essential for bone formation and matrix production in bone and is expressed from the early stages of differentiation onwards [34]. All groups' cells showed a similar level of Col I mRNA expression at 10 and 20 days. This result was similar to that of the study which reported that a similar level of Col I mRNA expression was shown in Aligpore, Bio-Oss and PepGen P-15 cultured on day 6 and 21 [35]. OPN is also a marker for osteoblastic differentiation and is expressed in the early stages as well as in the postproliferative period of osteoblastic growth [34]. Our investigations showed expression of OPN throughout the entire culture period in all groups. However, the expression of OPN was lowest in all the groups cultured on day 30. It was considered that differentiation of osteoblasts almost terminated at this period. The regulation of OPN expression correlates with bone development where an increase in an osteopontin expression level reduces proliferation as well as induces differentiation of osteoblasts [36-38]. Among the experimental groups, the highest expression of osteopontin mRNA was observed in the group cultured with ABM/P-15, followed by those with ABM/T-CAM and ABM on day 20, the periods between the bone matrix formation/maturation and mineralization stages. Our results support the idea that ABM/T-CAM and ABM/P-15 provide an appropriate environment for MC3T3-E1 cells to undergo differentiation into mature osteoblasts. This implies that the biomimetic surface of ABM/T-CAM and ABM/P-15 was involved not only in cell proliferation but also in regulation of cellular differentiation.

The growth and mineralization pattern of osteoblast-like cells cultured with ABM, ABM/T-CAM, and ABM/P-15 was examined by staining with alizarin red S at 30 day culture. The halo of red staining around the isolated ABM/T-CAM and ABM/P-15 particles was wider than that around the ABM. This pattern was similar to a study reporting that a halo of

red stain consistent with Ca^{2+} deposition can be seen in human gingival fibroblast matrix associated with ABM/P-15 [29]. The presence of a halo stain surrounding ABM particles can be deduced to be associated with a newly mineralized matrix produced by the cells. Therefore, the marked stain associated with the 3-D cellular colony on the surface of ABM/T-CAM and ABM/P-15 particles indicated that ABM/T-CAM and ABM/P-15 particles could induce more mineralization than ABM particles. The interparticular bridges comprised of cells were seen in ABM, ABM/T-CAM, and ABM/P-15 cultures, but it was much more intense and frequent in ABM/T-CAM and ABM/P-15 cultures. The cells in these bridges play a major role in the clustering of particles by generating tractional forces. Mechanical stimulation stimulates bone formation and inhibits bone resorption in cultured bone tissue and cells [39].

Mechanical stimulation induced by biomimetic surfaces of ABM/T-CAM and ABM/P-15 might increase the mineralization of osteoblast-like cells.

In this study, ABM/T-CAM seemed to have similar bone forming bioactivity compared to ABM/P-15 *in vivo*. A complete bony bridge was seen in two thirds of defects in the ABM/T-CAM and ABM/P-15 groups on week 4. These results corresponded to the hypothesis that a recombinant P-15 binding domain was a prerequisite for a multifocal formation of new bone in the defect filled with PepGen P-15, where the new bone was not organized exclusively starting from vital bone walls unlike the classical defect healing process [40]. These findings indicated that the cell-binding peptides of type I collagen and synthetic peptide related to cell adhesion contributed to favorable new bone formation.

The data presented here support our hypothesis that immobilizing T-CAM, composed of four cell adhesion molecules (RGD, PHSRN in fibronectin and EPDIM, YH in β ig-h3) on ABM, will enhance the ability of the ceramic matrix to serve as a host for osteoblast-like cells. The ability of ABM/T-CAM is similar to that of ABM/P-15.

In conclusion, ABM/T-CAM, which seemed to have similar bone forming bioactivity to ABM/P-15, was found to serve as an effective tissue-engineered bone graft material.

CONFLICT OF INTEREST

No potential conflict of interest relevant to this article was reported.

ACKNOWLEDGEMENTS

This work was supported by a grant (code #:10033799-2009-11) from "The Industry Original Technology Development

Project' funded by the Ministry of Knowledge Economy, Republic of Korea.

REFERENCES

- Boyne PJ. Induction of bone repair by various bone grafting materials. In: Ciba Foundation, editor. Hard tissue growth, repair and remineralization. Ciba Foundation Symposium 11. New York: Elsevier; 1973. p.121-41.
- Burchardt H. The biology of bone graft repair. *Clin Orthop Relat Res* 1983;174:28-42.
- Urist MR. Bone: formation by autoinduction. 1965. *Clin Orthop Relat Res* 2002;395:4-10.
- Qian JJ, Bhatnagar RS. Enhanced cell attachment to anorganic bone mineral in the presence of a synthetic peptide related to collagen. *J Biomed Mater Res* 1996;31:545-54.
- Scaria PV, Sorensen KR, Bhatnagar RS. Expression of a reactive molecular perspective within the triple helical region of collagen. 11st American Peptide Symposium. Albuquerque: American Peptide Society; 1989. p.605-7.
- Bhatnagar RS, Qian JJ, Gough CA. The role in cell binding of a beta-bend within the triple helical region in collagen alpha 1 (I) chain: structural and biological evidence for conformational tautomerism on fiber surface. *J Biomol Struct Dyn* 1997;14:547-60.
- Bhatnagar RS, Qian JJ, Wedrychowska A, Sadeghi M, Wu YM, Smith N. Design of biomimetic habitats for tissue engineering with P-15, a synthetic peptide analogue of collagen. *Tissue Eng* 1999;5:53-65.
- Nguyen H, Qian JJ, Bhatnagar RS, Li S. Enhanced cell attachment and osteoblastic activity by P-15 peptide-coated matrix in hydrogels. *Biochem Biophys Res Commun* 2003; 311:179-86.
- Barboza EP, de Souza RO, Caúla AL, Neto LG, Caúla Fde O, Duarte ME. Bone regeneration of localized chronic alveolar defects utilizing cell binding peptide associated with anorganic bovine-derived bone mineral: a clinical and histological study. *J Periodontol* 2002;73:1153-9.
- Tehemar S, Hanes P, Sharawy M. Enhancement of osseointegration of implants placed into extraction sockets of healthy and periodontally diseased teeth by using graft material, an ePTFE membrane, or a combination. *Clin Implant Dent Relat Res* 2003;5:193-211.
- Thorwarth M, Schultze-Mosgau S, Wehrhan F, Kessler P, Srouf S, Wiltfang J, et al. Bioactivation of an anorganic bone matrix by P-15 peptide for the promotion of early bone formation. *Biomaterials* 2005;26:5648-57.
- Park JW, Lee SG, Choi BJ, Suh JY. Effects of a cell adhesion molecule coating on the blasted surface of titanium implants on bone healing in the rabbit femur. *Int J Oral Maxillofac Implants* 2007;22:533-41.
- Pytela R, Pierschbacher MD, Ruoslahti E. Identification and isolation of a 140 kd cell surface glycoprotein with properties expected of a fibronectin receptor. *Cell* 1985;40: 191-8.
- Ruoslahti E, Pierschbacher MD. New perspectives in cell adhesion: RGD and integrins. *Science* 1987;238:491-7.
- Verrier S, Pallu S, Bareille R, Jonczyk A, Meyer J, Dard M, et al. Function of linear and cyclic RGD-containing peptides in osteoprogenitor cells adhesion process. *Biomaterials* 2002;23:585-96.
- Aota S, Nomizu M, Yamada KM. The short amino acid sequence Pro-His-Ser-Arg-Asn in human fibronectin enhances cell-adhesive function. *J Biol Chem* 1994;269: 24756-61.
- Skonier J, Bennett K, Rothwell V, Kosowski S, Plowman G, Wallace P, et al. Beta ig-h3: a transforming growth factor-beta-responsive gene encoding a secreted protein that inhibits cell attachment in vitro and suppresses the growth of CHO cells in nude mice. *DNA Cell Biol* 1994;13:571-84.
- Kawamoto T, Noshiro M, Shen M, Nakamasu K, Hashimoto K, Kawashima-Ohya Y, et al. Structural and phylogenetic analyses of RGD-CAP/beta ig-h3, a fasciclin-like adhesion protein expressed in chick chondrocytes. *Biochim Biophys Acta* 1998;1395:288-92.
- Kim JE, Kim SJ, Lee BH, Park RW, Kim KS, Kim IS. Identification of motifs for cell adhesion within the repeated domains of transforming growth factor-beta-induced gene, betaig-h3. *J Biol Chem* 2000;275:30907-15.
- Kim JE, Jeong HW, Nam JO, Lee BH, Choi JY, Park RW, et al. Identification of motifs in the fasciclin domains of the transforming growth factor-beta-induced matrix protein betaig-h3 that interact with the alphavbeta5 integrin. *J Biol Chem* 2002;277:46159-65.
- Krammer A, Craig D, Thomas WE, Schulten K, Vogel V. A structural model for force regulated integrin binding to fibronectin's RGD-synergy site. *Matrix Biol* 2002;21:139-47.
- Bodine PV, Green J, Harris HA, Bhat RA, Stein GS, Lian JB, et al. Functional properties of a conditionally phenotypic, estrogen-responsive, human osteoblast cell line. *J Cell Biochem* 1997;65:368-87.
- Franceschi RT. The developmental control of osteoblast-specific gene expression: role of specific transcription factors and the extracellular matrix environment. *Crit Rev Oral Biol Med* 1999;10:40-57.
- Hynes RO. Integrins: versatility, modulation, and signaling in cell adhesion. *Cell* 1992;69:11-25.
- Clover J, Dodds RA, Gowen M. Integrin subunit expression by human osteoblasts and osteoclasts in situ and in culture. *J Cell Sci* 1992;103(Pt 1):267-71.

26. Gronthos S, Stewart K, Graves SE, Hay S, Simmons PJ. Integrin expression and function on human osteoblast-like cells. *J Bone Miner Res* 1997;12:1189-97.
27. Gronthos S, Simmons PJ, Graves SE, Robey PG. Integrin-mediated interactions between human bone marrow stromal precursor cells and the extracellular matrix. *Bone* 2001;28:174-81.
28. Saito T, Albelda SM, Brighton CT. Identification of integrin receptors on cultured human bone cells. *J Orthop Res* 1994;12:384-94.
29. Bhatnagar RS, QiannJJ, Anna Wedychowska A, Dixon E, Smith N. Biomimetic habitats for cells: ordered matrix deposition and differentiation in gingival fibroblasts cultured on hydroxyapatite coated with a collagen analogue. *Cell Mater* 1999;9:93-104
30. Krauser JT, Rohrer MD, Wallace SS. Human histologic and histomorphometric analysis comparing OsteoGraf/N with PepGen P-15 in the maxillary sinus elevation procedure: a case report. *Implant Dent* 2000;9:298-302.
31. Kim TI, Jang JH, Chung CP, Ku Y. Fibronectin fragment promotes osteoblast-associated gene expression and biological activity of human osteoblast-like cell. *Biotechnol Lett* 2003;25:2007-11.
32. Choi JY, Lee BH, Song KB, Park RW, Kim IS, Sohn KY, et al. Expression patterns of bone-related proteins during osteoblastic differentiation in MC3T3-E1 cells. *J Cell Biochem* 1996;61:609-18.
33. Genge BR, Sauer GR, Wu LN, McLean FM, Wuthier RE. Correlation between loss of alkaline phosphatase activity and accumulation of calcium during matrix vesicle-mediated mineralization. *J Biol Chem* 1988;263:18513-9.
34. Ignatius A, Blessing H, Liedert A, Schmidt C, Neidlinger-Wilke C, Kaspar D, et al. Tissue engineering of bone: effects of mechanical strain on osteoblastic cells in type I collagen matrices. *Biomaterials* 2005;26:311-8.
35. Turhani D, Weissenböck M, Watzinger E, Yerit K, Cvinkl B, Ewers R, et al. In vitro study of adherent mandibular osteoblast-like cells on carrier materials. *Int J Oral Maxillofac Surg* 2005;34:543-50.
36. Iseki S, Wilkie AO, Heath JK, Ishimaru T, Eto K, Morriss-Kay GM. Fgfr2 and osteopontin domains in the developing skull vault are mutually exclusive and can be altered by locally applied FGF2. *Development* 1997;124:3375-84.
37. Iseki S, Wilkie AO, Morriss-Kay GM. Fgfr1 and Fgfr2 have distinct differentiation- and proliferation-related roles in the developing mouse skull vault. *Development* 1999;126:5611-20.
38. Park MH, Shin HI, Choi JY, Nam SH, Kim YJ, Kim HJ, et al. Differential expression patterns of Runx2 isoforms in cranial suture morphogenesis. *J Bone Miner Res* 2001;16:885-92.
39. Kubota T, Yamauchi M, Onozaki J, Sato S, Suzuki Y, Sodek J. Influence of an intermittent compressive force on matrix protein expression by ROS 17/2.8 cells, with selective stimulation of osteopontin. *Arch Oral Biol* 1993;38:23-30.
40. Valentin AH, Weber J. Receptor technology--cell binding to P-15: a new method of regenerating bone quickly and safely-preliminary histomorphometrical and mechanical results in sinus floor augmentations. *Keio J Med* 2004;53:166-71.